

We are IntechOpen, the world's leading publisher of Open Access books Built by scientists, for scientists

6,900

Open access books available

186,000

International authors and editors

200M

Downloads

Our authors are among the

154

Countries delivered to

TOP 1%

most cited scientists

12.2%

Contributors from top 500 universities



WEB OF SCIENCE™

Selection of our books indexed in the Book Citation Index
in Web of Science™ Core Collection (BKCI)

Interested in publishing with us?
Contact book.department@intechopen.com

Numbers displayed above are based on latest data collected.
For more information visit www.intechopen.com



Formation of Sand Spit and Bay Barrier

Takaaki Uda, Masumi Serizawa and Shiho Miyahara

Abstract

The formation of a sand spit and bay barrier was predicted using the BG model, covering three topics: (1) formation of a bay barrier in flat shallow sea and merging of bay mouth sand spits (Section 2), (2) elongation of a sand spit on a seabed with different water depths (Section 3), and (3) deformation of a sandbar formed at the tip of the Futtsu cusped foreland owing to a tsunami which propagated into Tokyo Bay after the Great East Japan Earthquake on March 11, 2011 (Section 4). The Type 5 BG model was employed in Section 2, and Type 3 BG model in Sections 3 and 4.

Keywords: sand spit, bay barrier, embayed coasts, Futtsu cusped foreland

1. Introduction

A barrier island normally develops along the marginal area of a flat shallow sea. Various explanations have been given for the cause of the development of barrier islands: the elongation of a sand spit, the emergence of a longshore bar during the decreasing sea level, and the submergence of a beach ridge during the increasing sea level [1]. Nummedal [2] studied the physical process of the formation of a barrier island and concluded that it is closely related to four factors: the increase in the sea level during the past several thousand years, the longshore distribution of the sand source and the loss of sand, the exchange of sea water across inlets, and the wave energy level. However, the theoretical explanation for the growth of barrier islands as a result of extension of a sand spit was inadequate, and in particular, the effect of the change in water depth to the development of a barrier island was not fully investigated. In Section 2, therefore, this issue was focused. Among the various forms of barrier islands, a bay barrier [3] was taken as an example.

Zenkovich [4] gave an example of a barrier beach closing the bay mouth in a fjord in eastern Kamchatka. The elongation of a sand spit is commonly observed at bay or river mouths, where the direction of the shoreline abruptly changes. Consider a case in which the sand source is located on both sides of a bay. In this case, sand spits are formed near the mouth of a bay by the deposition of sand supplied from upcoast. When the water depth of the bay is sufficiently small, the sandbars can rapidly extend to form a bay barrier enclosing the bay. When the shape of the bay is asymmetrical, the sand spit located offshore has a wave-sheltering effect on the other spit, affecting the topographic changes of the other sand spit, and finally the two spits may merge. Taking these effects into account, the elongation and merging of sand spits at a bay mouth were studied using the Type 5 BG model in Section 2 [5].

Serizawa and Uda [6] predicted the development of a sand spit using the BG model, and their results were compared with the results of a movable-bed experiment. They successfully explained the formation of a sand spit and a barrier. In their study, however, the effects of the change in water depth of the sand accumulation zone on the formation of the sand spit have not yet been fully investigated. Taking a sand spit and a barrier formed along the west Izu coast in Suruga Bay as the example, these issues were investigated in Section 3 [7].

A 2-m-height tsunami propagated into Tokyo Bay after the Great East Japan Earthquake occurred on March 11, 2011, and a cusped foreland separating Tokyo Bay and the Uraga Strait was eroded by the current during this tsunami. Although this cusped foreland has long been stable, decreased sand supply from the south coast has resulted in erosion of the cusped foreland [8], and the previously straight sandbar had become concave northward with several openings by February 3, 2011 [9]. Then, the tsunami flowed over the sandbar, dispersing the sand and leaving an isolated protruding sandbar. After the tsunami, this sandbar was significantly deformed owing to wave action. The subsequent shoreline changes of this protruding sandbar were measured, and the 3-D beach changes were calculated and compared with the measured shoreline changes in Section 4 [9].

2. Numerical simulation of elongation and merging of bay mouth sand spits

2.1 Formation of bay barriers

Zenkovich [4] showed an example of a barrier beach in a fjord in eastern Kamchatka, which extended at the bay mouth (**Figure 1**). In this bay, downward longshore sand transport developed along the coastline, resulting in the formation of sand spits from both shores; they connected each other; and a barrier beach was formed. Note that the beach is wide at the central part of the bay barrier, whereas it is narrow at the right end. He gave another example of a sand spit formed in a bay mouth (**Figure 2**). **Figures 2A** and **2B** show the sand spits alternately extending from both shores of the bay mouth, and a slender sand spit extended owing to unidirectional longshore sand transport from the right bank, respectively. In another example of a pair of sand spits shown in **Figure 3**, the tips extended on both sides

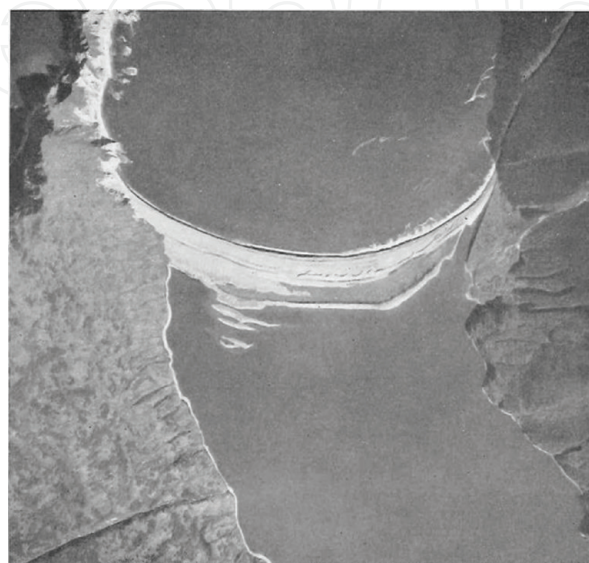


Figure 1.
Bay barrier closing bay mouth in fjord in eastern Kamchatka [4].

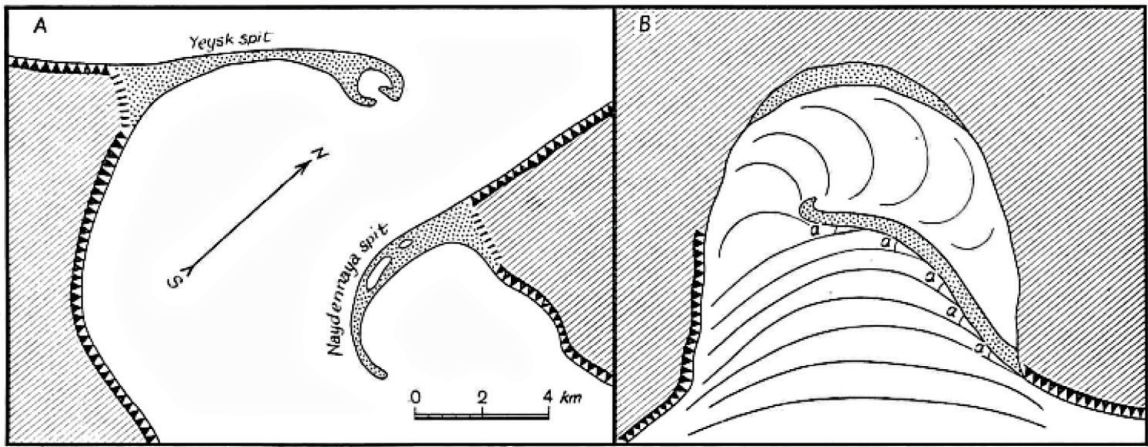


Figure 2.
Schematic diagram of formation of bay mouth sand spits [4].

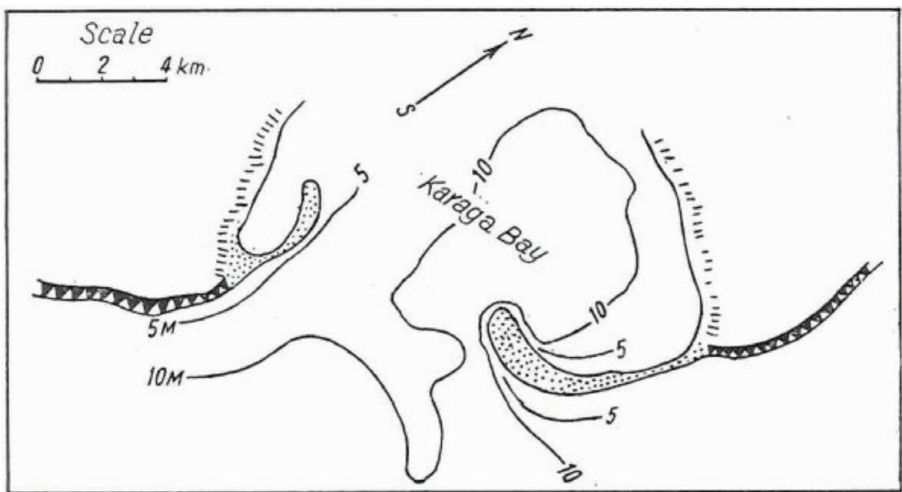


Figure 3.
Example of a pair of sand spits enclosing Karaga Bay [4].

of the bay markedly curved inward, because the water depth at the tips of the sand spits is too larger for the sand spits to extend in a straight line.

2.2 Calculation conditions

A rectangular calculation domain with 600 m length in the longshore and cross-shore directions was considered with a flat solid bed of 3 m depth, and sandy headlands with an initial beach slope of 1/10 and a berm height of 1 m were set at the left corner of this domain. Sand supplied from the headlands is available for the formation of a bay barrier. The beach changes were predicted when multidirectional irregular waves with a significant wave height of 1 m were incident from the direction normal to the y -axis, and the incident wave direction at each time step was randomly determined, so that the probability of occurrence of each wave direction was satisfied. As the probability of occurrence, the directional distribution of wave energy that corresponds to the angular spreading parameter $S_{\max} = 10$ for wind waves was used by employing the angular spreading method for irregular waves [10]. h_c and the equilibrium slope of sand were assumed to be 3 m and 1/10, respectively. **Table 1** summarizes the conditions for calculating the elongation and merging of bay mouth sand spits.

Four cases of calculation were carried out; a slender, rectangular sandy headland was placed at the left end of the calculation domain in Case 1, double sandy headlands with the same shape as that on the left side was placed in Case 2, and two

Calculation method	Type 5 BG model
Incident wave height H	1 m
Berm height h_R	1 m
Depth of closure h_c	3 m
Equilibrium slope $\tan \beta_c$	1/10
Coefficients of sand transport	Longshore and cross-shore sand transport coefficient $K_s = 0.2$
Mesh size	$\Delta x = \Delta y = 10$ m
Time interval	$\Delta t = 1$ hrs
Duration of calculation	2×10^4 hrs (2×10^4 steps)
Boundary conditions	Shoreward and landward ends $q_x = 0$ Right and left boundaries $q_y = 0$

Table 1.
Conditions for calculating elongation and merging of bay mouth sand spits.

sandy headlands were placed asymmetrically in Case 3. Furthermore, in Case 4, the formation of a barrier island closing three bays was predicted.

2.3 Calculation results

2.3.1 Single sandy headland (Case 1)

Figure 4 shows the calculation results up to 5000 hr in Case 1. A spatial imbalance in longshore sand transport occurred near the corner, causing erosion to the left of the corner, because waves were incident from the negative x -direction, and the shoreline orientation changed by 90° at the corner (**Figure 4(a)**). The eroded sand was transported rightward, resulting in the formation of sand spit A at the corner (**Figure 4(b)**). Simultaneously, shoreline undulation started to develop owing to the high-angle wave instability [11] along the shoreline extending parallel to the direction of wave propagation, and a small sand spit A' was formed. With time, the sand spit A was significantly elongated, producing a wave-shelter zone on the lee of the sand spit (**Figure 4(c)**). Although sand spits independently developed near the head and foot of the sandy headland at the initial stage, the wave-sheltering effect of sand spit A became dominant with increasing size of the sand spit, and the sand spit A' was subject to the wave-sheltering effect of sand spit A (**Figure 4(c)**). Finally, it disappeared, and sand spit A simply elongated rightward (**Figures 4(d), 4(e), and 4(f)**). This elongation of a single sand spit well explains the mechanism of the extension of sand spits given by Zenkovich [4], as schematically shown in **Figure 2**.

2.3.2 Deformation of symmetric sandy headlands on both sides of a bay (Case 2)

Figure 5 shows the results in Case 2, in which sandy headlands were symmetrically arranged on both sides of the bay with a distance of 320 m between them (**Figure 5(a)**). The sandy headland on the left, therefore, was subjected to the wave-sheltering effect from that on the right and vice versa. When waves were incident from the negative x -direction under these conditions, three small-scale sand spits had developed along the shoreline on both sides of the sandy headlands after 1000 hrs, together with the elongation of two slender sand spits, one on each side of the bay mouth (**Figure 5(b)**). By 2000 hrs, the two sand spits at the bay mouth had further extended, and the opening width was narrowed to 60 m (**Figure 5(c)**). Because waves were obliquely incident

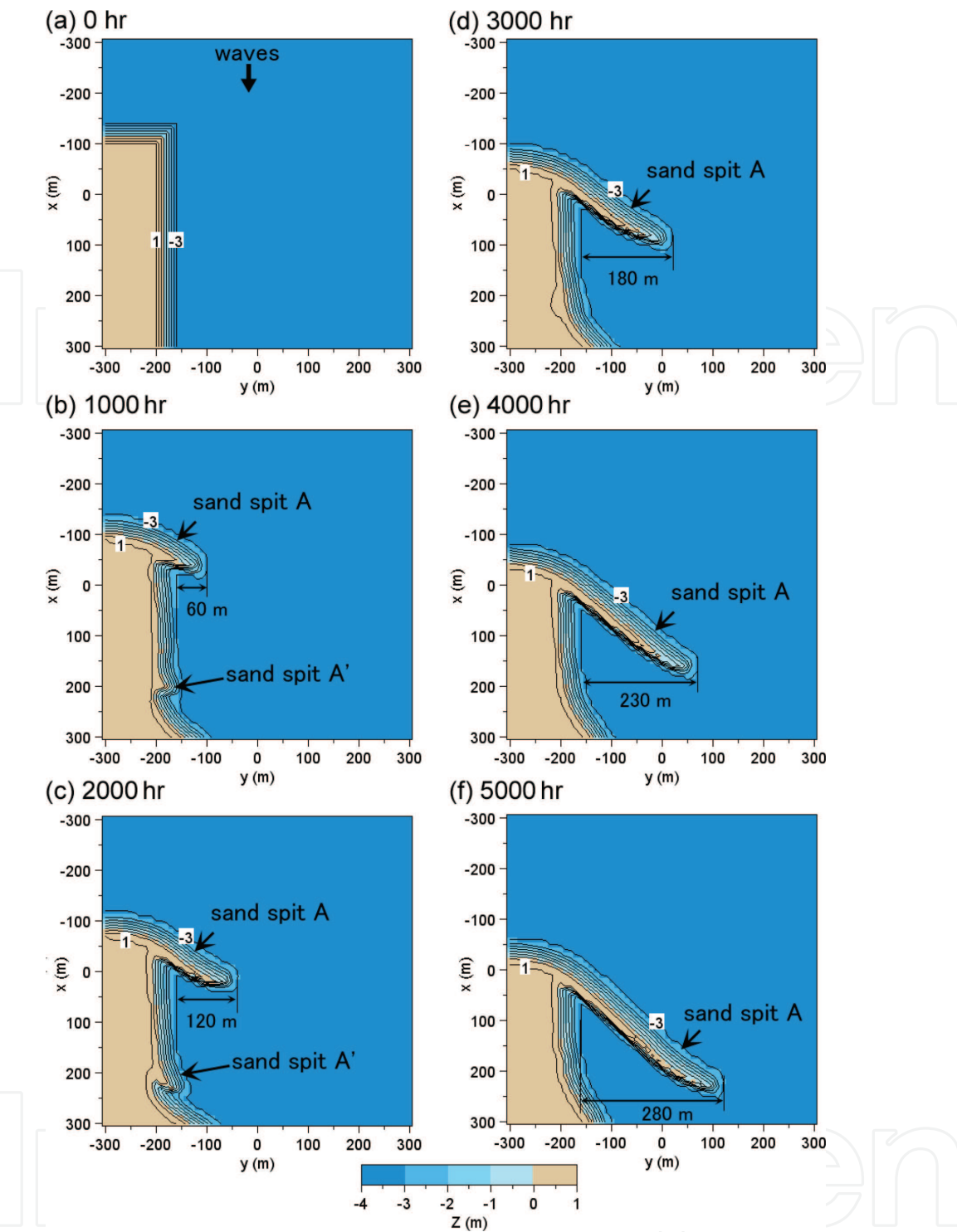


Figure 4.
Calculation results for elongation of sand spit along the shoreline on the right side of sandy headland (Case 1) [5].

to the sand spits on both sides of the sandy headlands through the opening, these sand spits further developed. The size of the three sand spits increased until 2000 hrs (**Figure 5(c)**). After 3000 hrs, the two sand spits that extended from both sides had connected to form a bay barrier. Because the bay mouth was completely closed by the bay barrier (**Figure 5(d)**), the sand spits that formed along the shoreline on both sides of the sandy headlands were left intact.

Longshore sand transport from the sandy headlands to the concave shoreline still prevailed even after the complete closure of the bay mouth by the bay barrier, and the beach width at the central part of the bay barrier increased with time (**Figures 5(e)-5(h)**). Comparing the shape of the bay barrier after 4000 hrs, as shown in **Figure 5(f)**, with **Figure 1**, the calculation results illustrating the

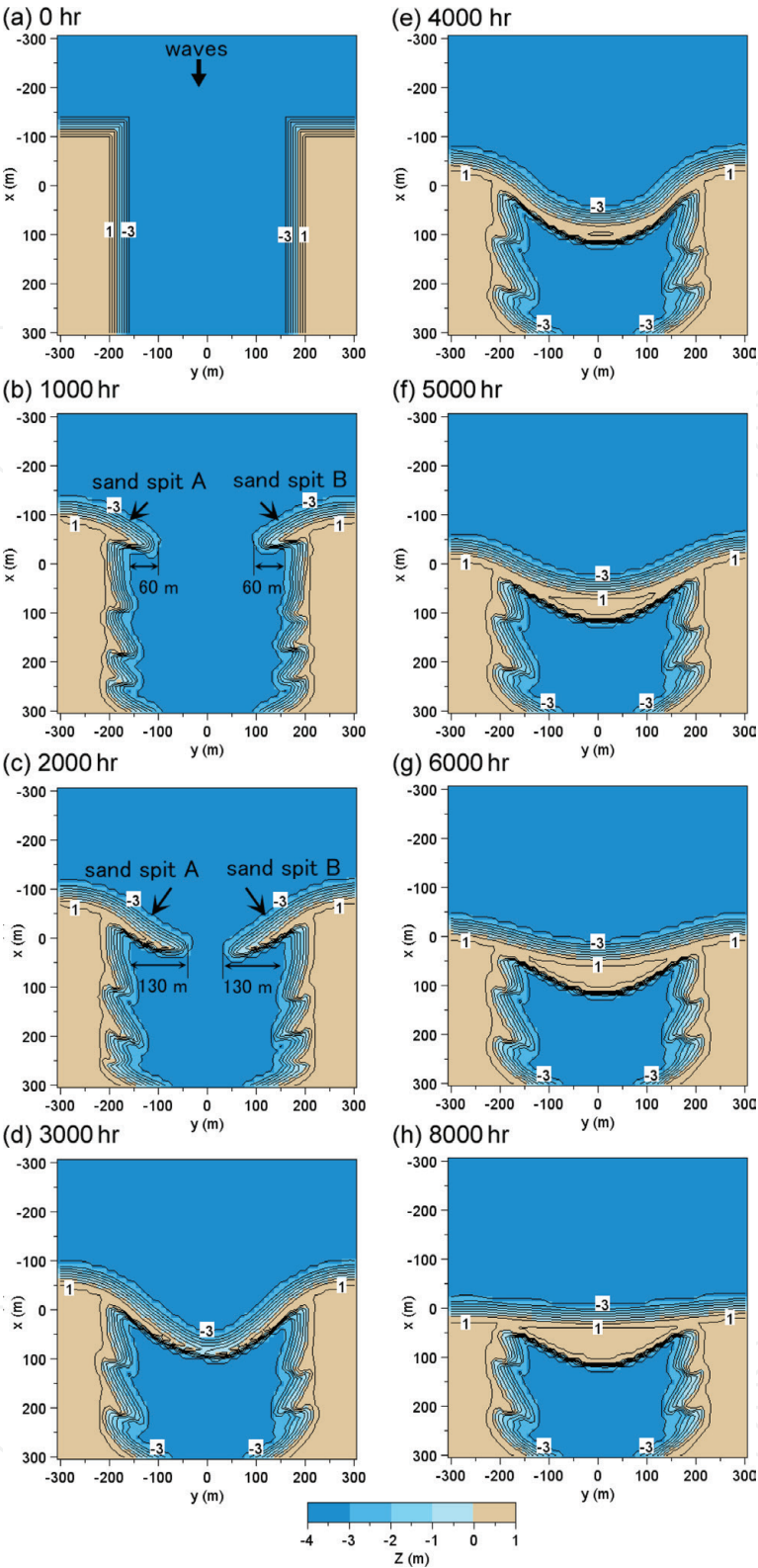


Figure 5. Calculation results for elongation of bay mouth bar between two sandy headlands separating a bay (Case 2: symmetric arrangement) [5].

development of a bay barrier and a wide beach at the central part of the bay barrier are in good agreement with the photograph in [4].

2.3.3 Deformation of asymmetric sandy headlands on both sides of a bay (Case 3)

When waves were incident from the negative x -direction, the wave-sheltering effect of the left sandy headland on the right headland became stronger because of the protrusion of the left headland (**Figure 6(a)**). After 1000 hrs, the sand spits had

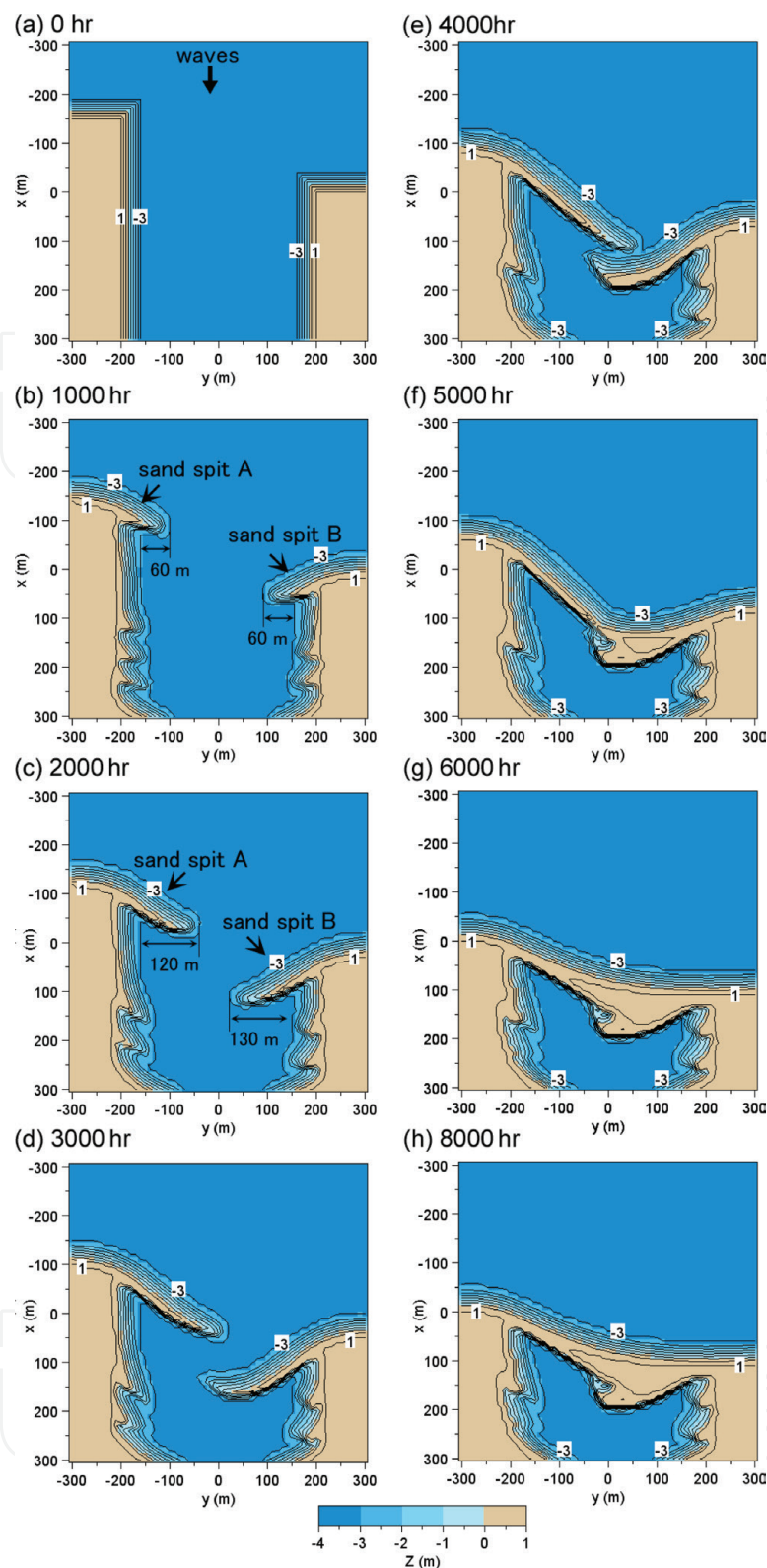


Figure 6.
Calculation results for elongation of bay mouth bar between two sandy headlands separating a bay (Case 3: asymmetric arrangement) [5].

started to form on both sides of the sandy headlands (**Figure 6(b)**). Here, the sand spits are denoted as sand spits A and B, respectively. At this stage, the elongation length of sand spits A and B was 60 m. With further wave action, sand spits A and B became markedly elongated to 120 and 130 m, respectively, after 2000 hrs (**Figure 6(c)**). Sand spit B was 10 m longer than sand spit A because of the larger wave-sheltering effect of sand spit A. After 3000 hrs, sand spit B had further elongated, and the tip of the sand spit curved and approached the tip of sand spit A (**Figure 6(d)**). After 4000 hrs, sand spit B had stopped elongating, because it had entered the wave-shelter

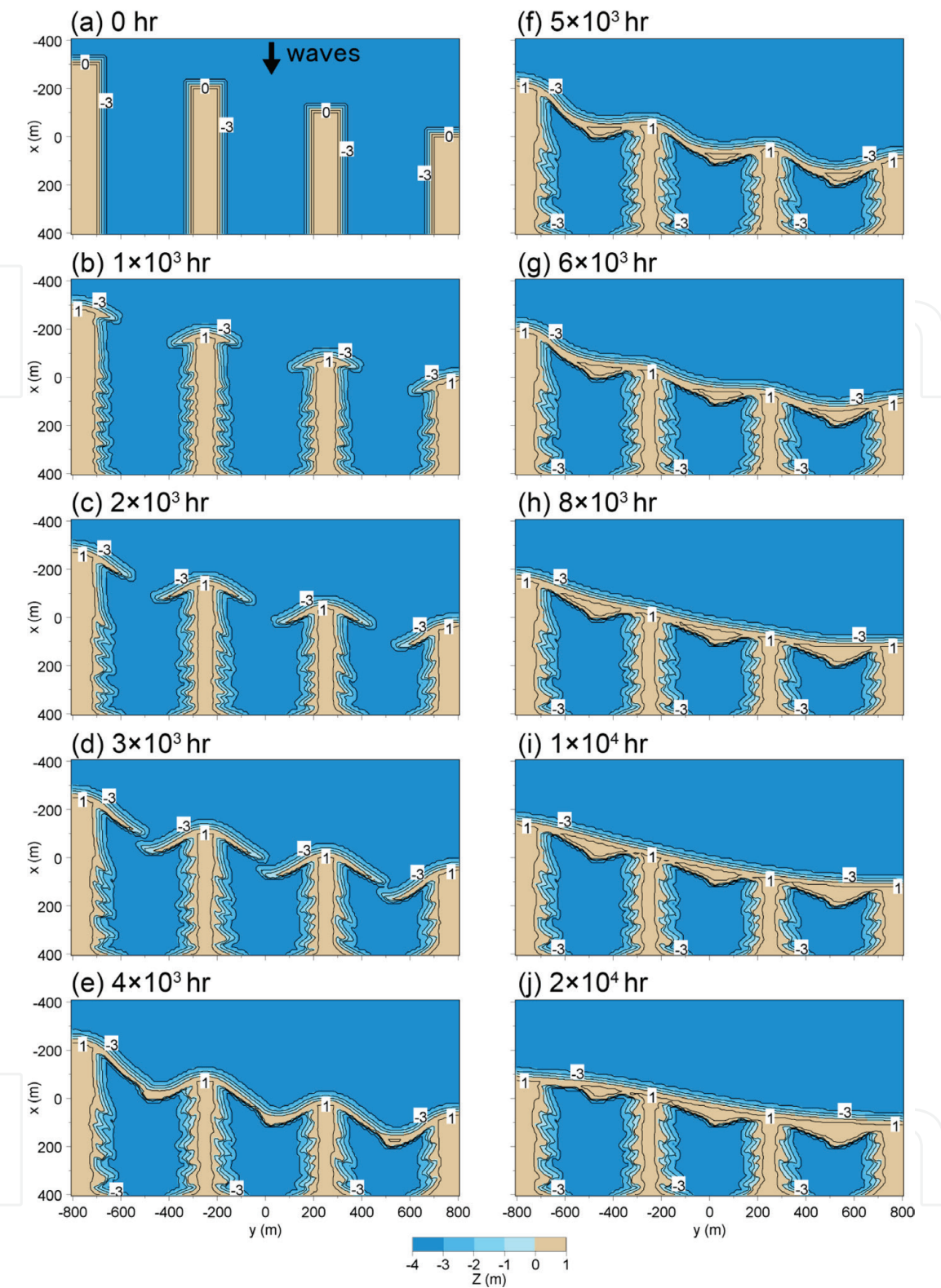


Figure 7.
Formation of embayed coasts closed by a barrier island (Case 4).

zone of sand spit A, and the tip of sand spit A became connected to sand spit B owing to successive sand deposition near the tip of sand spit A (**Figure 6(e)**). After 5000 hrs, a bay barrier had formed by the connection of the two sand spits A and B (**Figure 6(f)**). Because the shoreline protruded at this stage, the shoreline further retreated up to 8000 steps, and the shoreline inclination was reduced (**Figure 6(h)**).

In Case 3, the width of the bay increased by the deposition of sand at the tip of sand spit B, and a bay barrier with a wide shore in the central part was formed after 5000 hrs. With time, the bay barrier continued to develop up to 8000 hrs, although

a protrusion that had formed near the point connecting the two sand spits was left intact. This protrusion was formed when sand spit A was superimposed on sand spit B from the offshore side in the period between 4000 and 5000 hrs, which corresponds to the previous beach changes in the evolution process of the bay barrier.

2.3.4 Formation of embayed coasts by extension of a barrier island (Case 4)

Zenkovich [4] illustrated the main stages of the evolution of an embayed coast as in Figure 223 (p. 451) in his book and described that the process is as follows: the first stage is completed when the bays are cut off from the sea by barrier beaches which link up capes and peninsulas that have already retreated slightly as a result of abrasion. Then, as the next stage, all the projections have been cut away, and the coastline has advanced to the heads of the former bays.

In Case 4, the formation of the embayed coasts by the extension of a barrier island as described in Zenkovich [4] was predicted. At the initial stage, four headlands composed of sand were considered with three bays between these headlands, the length of which gradually decreases in the direction of the y -axis (**Figure 7(a)**). Waves were assumed to be incident from the negative x -direction. Successive topographic changes of the embayed coasts over time are shown in **Figure 7**. By 10^3 hrs, short sand spits started to extend from the tips of the headlands (**Figure 7(b)**). With time, these sand spits extended, and they connected each other and merged up to 4×10^3 hrs (**Figures 7(c), 7(d), and 7(e)**). Because the shoreline of the barrier islands protrudes in front of the headlands at these stages, such projections were eroded away owing to longshore sand transport, resulting in the formation of a straight coastline with time (**Figures 7(f)-7(i)**). Finally, three bays closed by a straight barrier island were formed (**Figure 7(j)**). These results are in good agreement with the explanation of the formation of the embayed coasts given by Zenkovich [4].

3. Numerical simulation of elongation of sand spit on seabed with different water depths

3.1 Examples of sand spit and barrier on west Izu coast

Typical examples of the sand spit and barrier can be seen on the west Izu coast (**Figures 8 and 9**) [7]. A recurved sand spit, Mihama Point, of 650 m length extends at the mouth of Heda Bay. The bathymetry in the rectangular area of Heda Bay in **Figure 9** is drawn in **Figure 10**. The water depth at the tip of the sand spit reaches 30 m, which is much greater than the depth of closure of $h_c = 10$ m in this area, and the slope around the tip of sand spit is very steep. Also, a barrier is located 2.2 km north of the sand spit (**Figures 9 and 11**), separating Myojin Pond from Suruga Bay, and further north, another recurved sand spit, Osezaki Point, of 650 m length extends 3.3 km north of the pond (**Figures 8 and 12**). The development of a sand spit and a barrier in these examples strongly suggests that the water depth of the sand deposition zone is a key factor for the formation of the sand spit and the barrier.

3.2 Calculation conditions

The water depths of the shallow seabed where the sand spit elongates were set to 5, 10, 15, and 20 cm in Cases 1–4, respectively, with a model scale of 1/100. The incident wave height was $H_i = 4.6$ cm, and the wave period $T = 1.27$ s. Waves were obliquely incident at an angle of 20° relative to the direction normal to the initial



Figure 8.
Location of Heda and Osezaki Points on the west coast of Izu Peninsula.

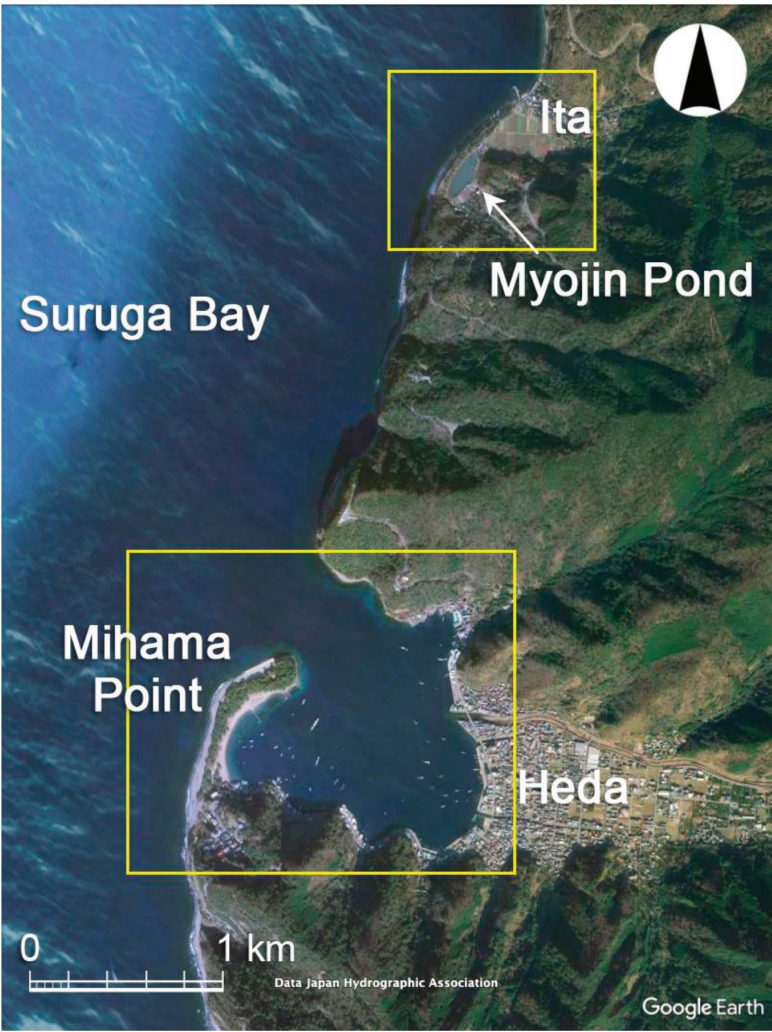


Figure 9.
Satellite image of Mihama Point and Myojin Pond.

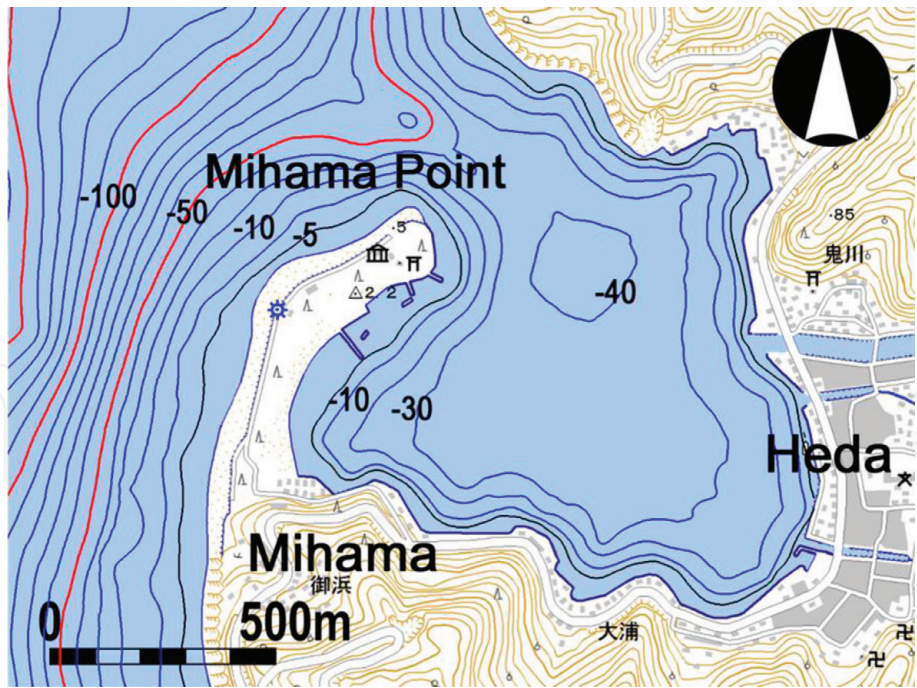


Figure 10.
Bathymetry around Mihama Point [7].



Figure 11.
Aerial photograph of Myojin Pond.

shoreline. The depth of closure was given as $h_c = 2.5H$, where H is the wave height at a point. h_R and the equilibrium slope of sand were assumed as 5 cm and 1/5, respectively, based on the experimental results. The calculation domain was discretized by meshes of 20 cm, and the 8 hrs of calculation (8×10^4 steps) was carried out using the time intervals of $\Delta t = 10^{-4}$ hr. **Table 2** summarizes the conditions for calculating the elongation of a sand spit. The calculation results are shown with the same model scale of 1/100, so that it is easy to compare the results of this study with those given in [6], in which the formation of a spit with a model scale of 1/100 was predicted. The numbers in parentheses in **Table 2** correspond to the experimental conditions.



Figure 12.
Aerial photograph of Osezaki Point taken in 2005.

Calculation method	Type 3 BG model
Wave conditions	Incident waves: $H_I = 4.6$ m (4.6 cm), $T = 12.7$ s (1.27 s), wave direction $\theta_I = 20^\circ$ relative to normal to initial shoreline
Berm height	$h_R = 5$ m (5 cm)
Depth of closure	$h_c = 2.5H$ (H : wave height)
Equilibrium slope	$\tan\beta_c = 1/5$
Angle of repose slope	$\tan\phi = 1/2$
Coefficients of sand transport	Coefficient of longshore sand transport $K_s = 0.045$ Coefficient of Ozasa and Brampton [12] term $K_2 = 1.62K_s$ Coefficient of cross-shore sand transport $K_n = 0.1 K_s$
Mesh size	$\Delta x = \Delta y = 20$ m (20 cm)
Time intervals	$\Delta t = 10^{-3}$ hr. (10^{-4} hr)
Duration of calculation	80 (8) hrs (8×10^4 steps)
Boundary conditions	Shoreward and landward ends, $q_x = 0$; right and left boundaries, $q_y = 0$
Calculation of wave field	Energy balance Equation [13] <ul style="list-style-type: none">• Term of wave dissipation due to wave breaking: Dally et al. [14]• Wave spectrum of incident waves: directional wave spectrum density obtained by Goda [15]• Total number of frequency components $N_F = 1$ and number of directional subdivisions $N_\theta = 8$• Directional spreading parameter $S_{\max} = 75$• Coefficient of wave breaking $K = 0.17$ and $\Gamma = 0.3$• Imaginary depth between minimum depth h_0 and berm height h_R: $h_0 = 2$ m (2 cm)• Wave energy = 0 where $Z \geq h_R$• Lower limit of h in terms of wave decay due to breaking Φ, 0.7 m (0.7 cm)

Table 2.
Conditions for calculating elongation of a sand spit.

3.3 Calculation results

3.3.1 Formation of sand spit on a flat bottom with constant depth

Figures 13–16 show the initial topographies with a flat bottom in the sand deposition area and the results after an 8-hr wave action of Cases 1–4. In Case 1 (Figure 13), a sand spit rapidly extended along the marginal line of the shallow seabed forming a barrier (Figure 13(b) and 13(c)), because the water depth of the sand deposition zone is much smaller than the depth of closure h_c of 12 cm, and it connected with the other side, leaving a shallow lagoon inside up to 2 hrs (Figure 13(d)). After 4 hrs, the width of the sandbar increased because of the sand deposition to the deeper zone from the left boundary while forming a steep slope (Figure 13(e)).

In Case 2 ($h_0 = 10$ cm, Figure 14), the elongation velocity of the sand spit decreased compared with that in Case 1 because of the increase in the volume of the sand deposition zone. Simultaneously, the curvature of the shoreline at the tip

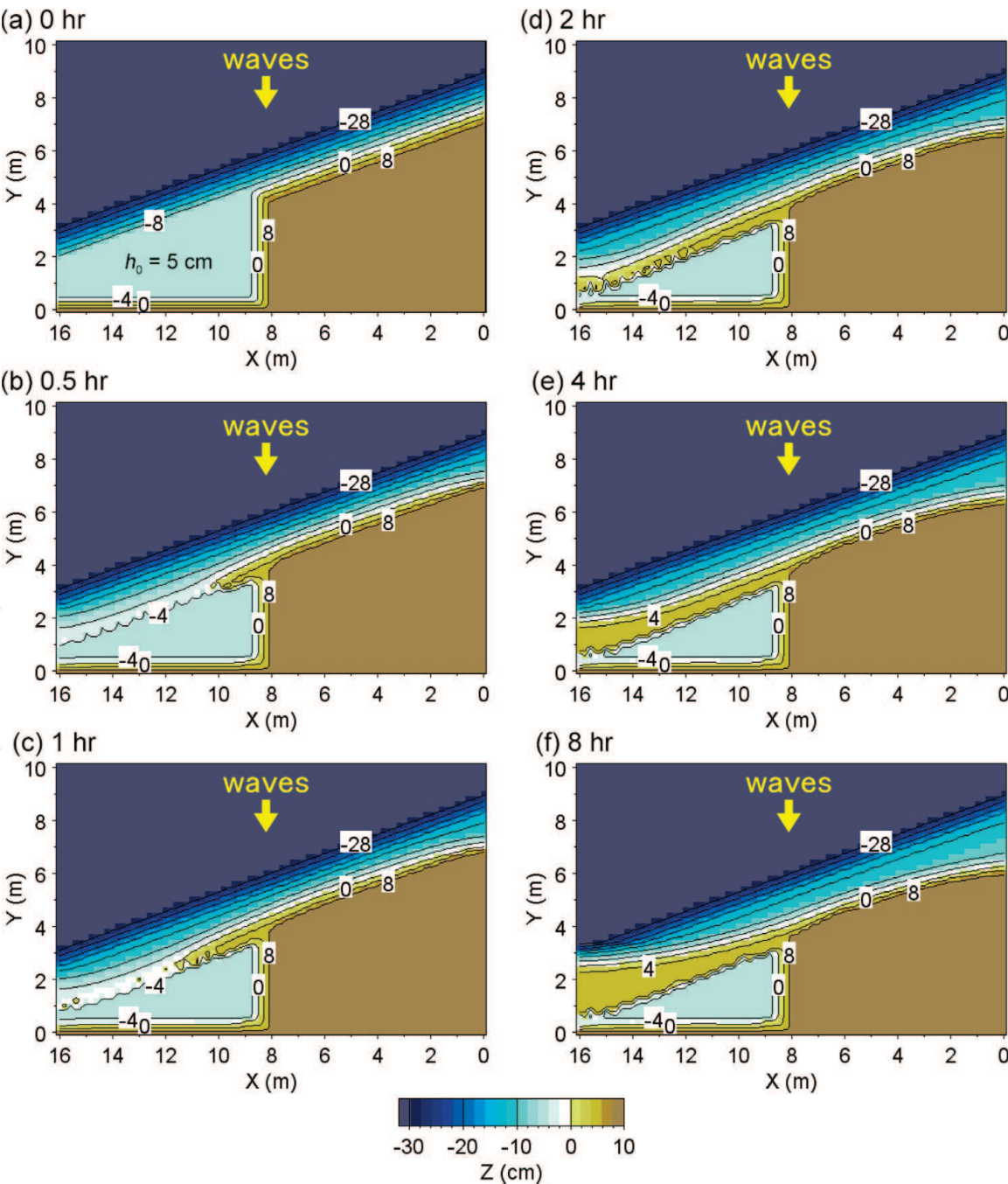


Figure 13.
Formation of sand spit on the flat seabed with 5 cm depth in Case 1 [7].

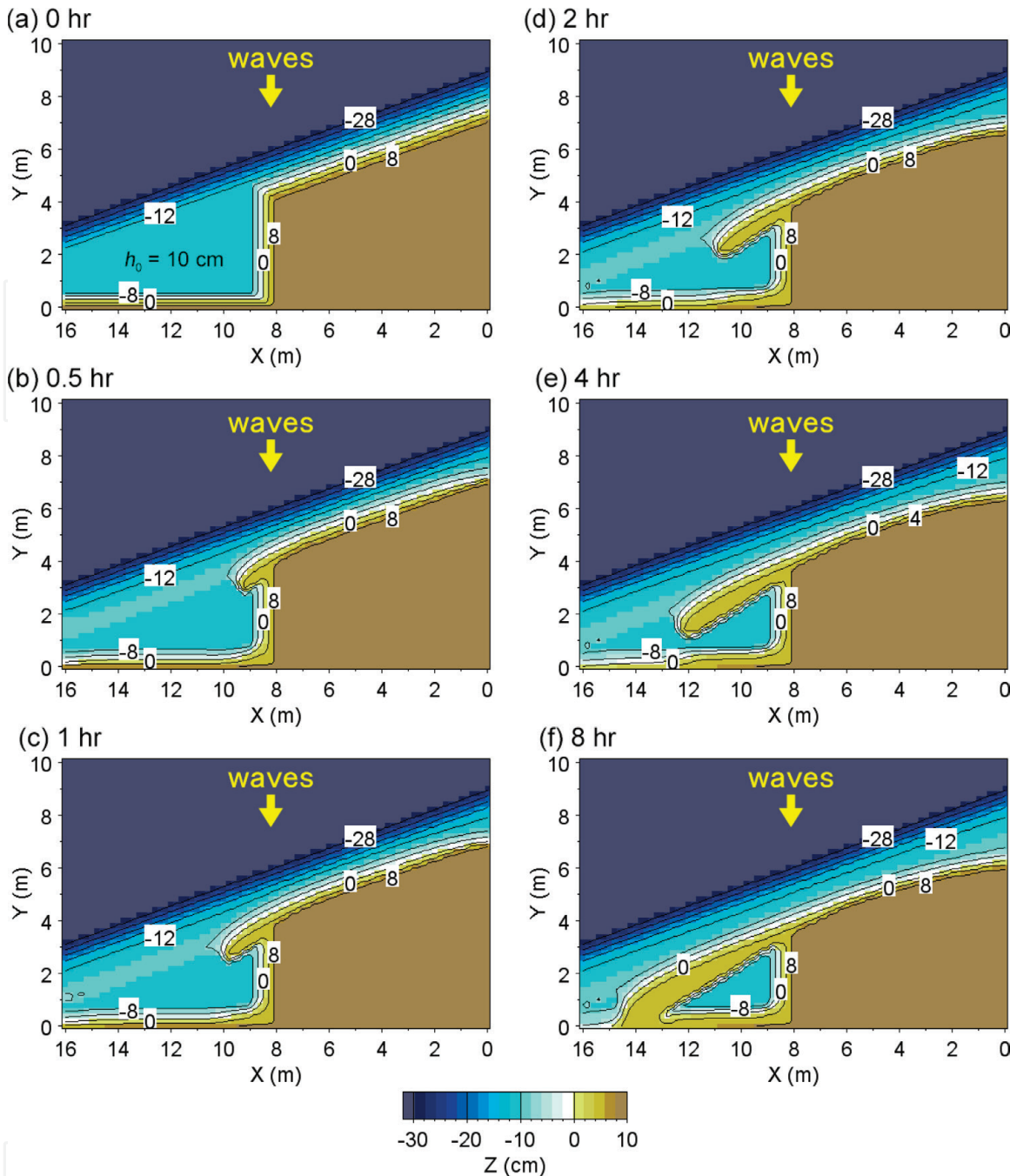


Figure 14. Formation of sand spit on the flat seabed with 10 cm depth in Case 2 [7].

of the sand spit increased because of the larger wave energy incident to the shallow seabed (**Figures 14(b), 14(c), and 14(d)**). As a result, the tip of the sand spit approached very close to the X-axis after 4 hrs and connected at $X = 14$ m after 8 hrs (**Figures 14(e) and 14(f)**). A cusate foreland was formed on the opposite side against the sand spit after 4 hrs owing to the wave-sheltering effect of the sand spit, and the area of the lagoon behind the barrier markedly decreased in Case 2 compared with that in Case 1.

In Case 3 ($h_0 = 15$ cm, **Figure 15**), the elongation velocity and the length of the sand spit further decreased because of successive sand deposition into the deeper zone. When the water depth of a flat bottom is greater than h_c , part of the sand transported from upcoast falls into the zone deeper than h_c , and such sand cannot be transported again by wave action (**Figures 15(b), 15(c), and 15(d)**), implying that an additional volume of sand is required for the sand spit to extend. It is concluded that the greater the water depth of a flat bottom, the slower the development

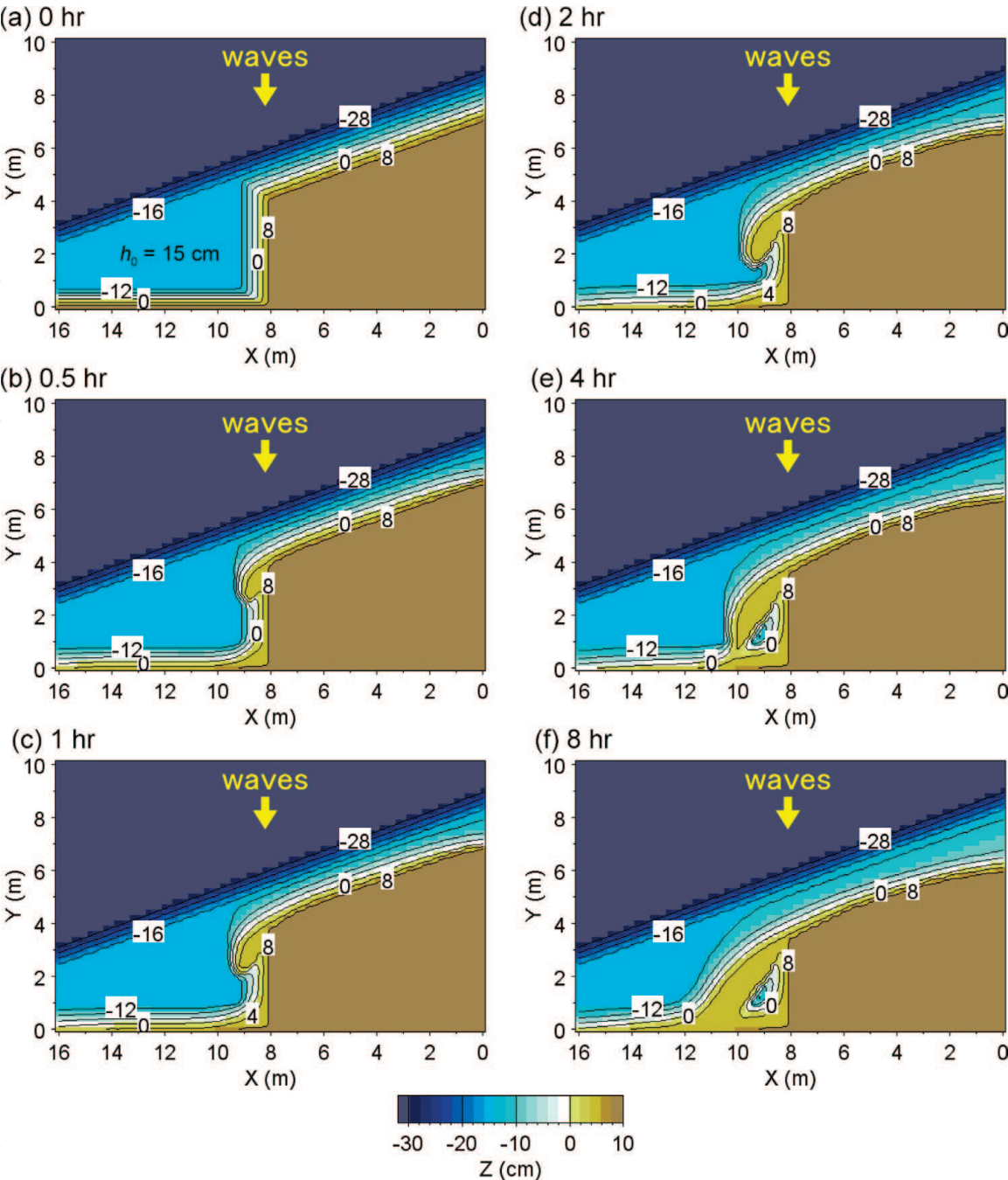


Figure 15.
Formation of sand spit on the flat seabed with 15 cm depth in Case 3 [7].

of a sand spit, even if the same amount of sand is supplied from the upcoast. With the increase in the water depth of the flat bottom, the tip of the sand spit was forced to be bent landward. Moreover, the sand deposited upcoast of the sand spit quickly discharged downcoast after 4 hrs, because the shoreline at the tip of the sand spit smoothly connected to the opposite shore, so that longshore sand transport was able to smoothly reach the downcoast shoreline ((**Figure 15(e)**)).

In Case 4 ($h_0 = 20$ cm, **Figure 16**), the development of the sand spit was depressed, and its size was reduced. Although a small hollow was formed behind the sandbar, no lagoon was formed (**Figures 16(b)-16(e)**). **Figure 17** shows the shoreline configurations in Cases 1–4 after 2 hrs. The shoreline upcoast of $X = 8$ m, i.e., sand source, coincides with each other, suggesting that equivalent longshore sand transport develops in each case. Thus, it is concluded that the sand spit was formed under the condition that a constant volume of sand is supplied from the upcoast. In other words, the difference in the development of the sand spit must be

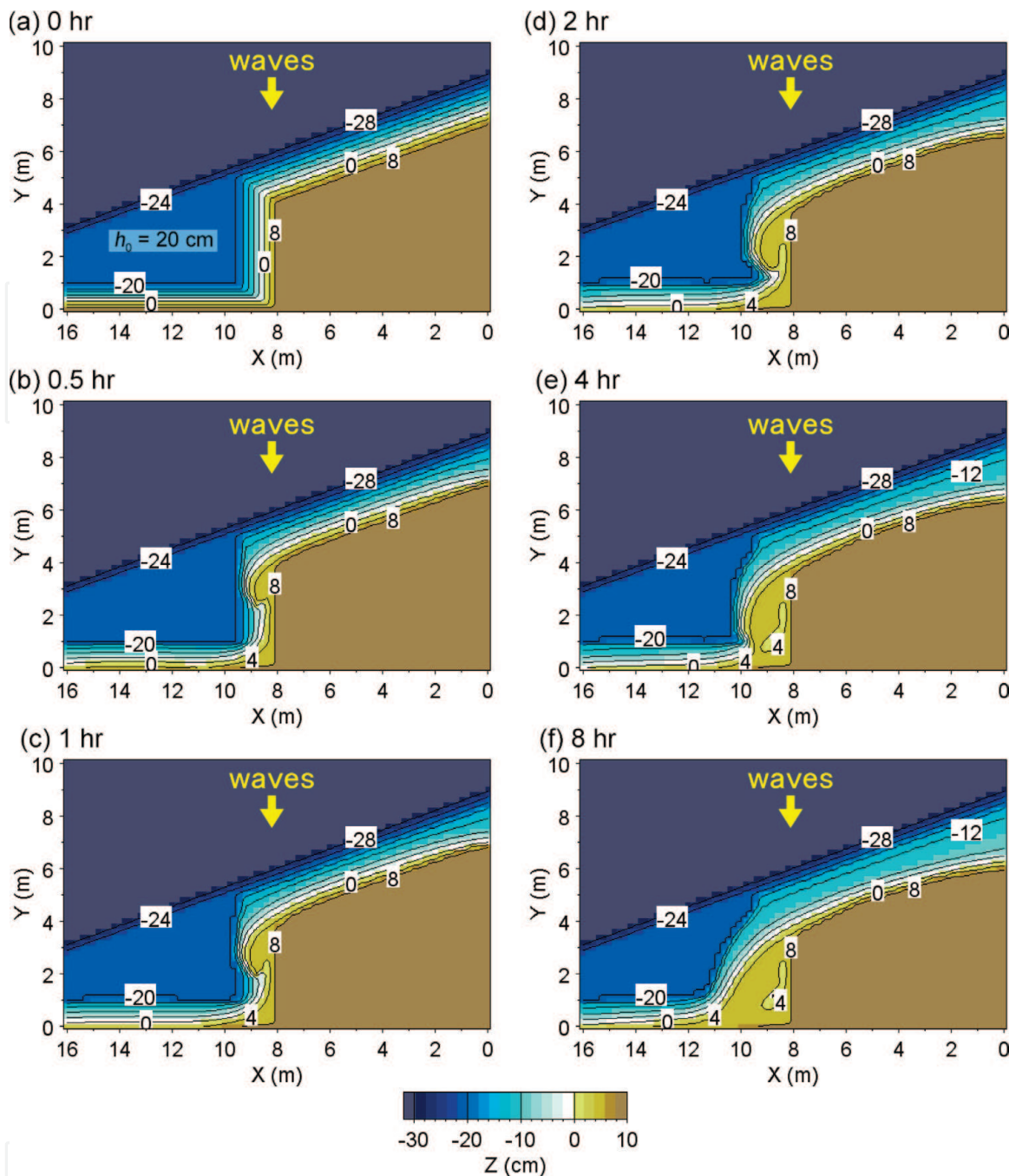


Figure 16. Formation of sand spit on the flat seabed with 20 cm depth in Case 4 [7].

explained only by the difference in the water depth. With the increase in the water depth, the sand spit was depressed, and a semicircular cusped foreland was formed instead of a sand spit when the water depth of the flat shallow seabed is 20 cm.

3.4 Discussion

When a constant longshore sand transport Q_0 is supplied from upcoast and a sand spit is formed owing to this sand supply, the elongation velocity of the sand spit is proportional to Q_0/h^2 , where h is the water depth of the sand deposition area. The development of the sand spit is remarkable with a smaller water depth of the sand deposition zone. At the same time, sufficient wave energy cannot reach deep into the shallow body of water, inducing the development of a sandbar there, whereas sufficient wave energy can reach the shoreline with a larger water depth, resulting in the increase in the curvature of the shoreline. Mihama Point with a

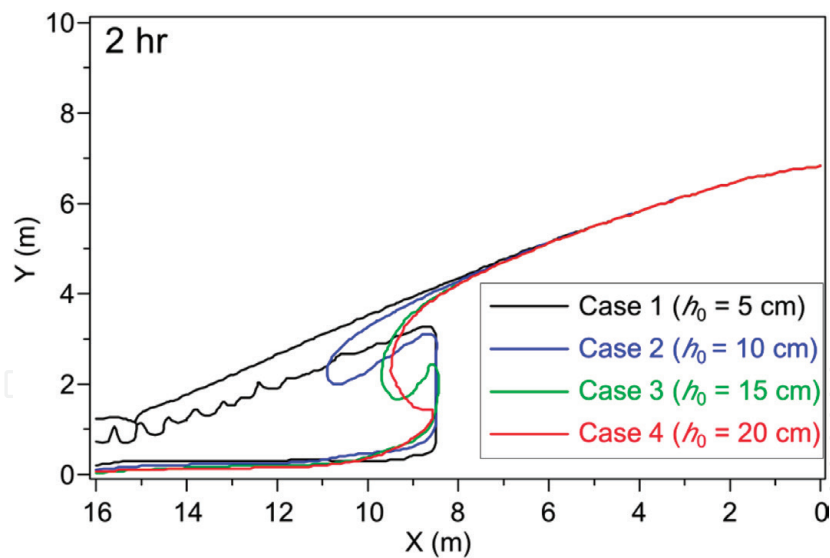


Figure 17.
 Shoreline configurations after 2 hrs for Cases 1–4 [7].

large water depth of the sand deposition area, which is much larger than the depth of closure h_c of 10 m, as shown in **Figure 10**, is very similar to the results after 2 hrs in Case 3 (**Figure 15(d)**). The topography of Myojin Pond (**Figure 11**) is similar to that after 8 hrs in Case 2 (**Figure 14(f)**), implying that Myojin Pond was left behind as a shallow pond, as a result of the extension of a barrier island. In case of Osezaki Point that protruded northward at the north end of Izu Peninsula (**Figure 12**), the sand spit extended straight from the turning point of the coastline, and then the tip of the sand spit recurved inward. This feature is similar to the result after 2 hrs in Case 2 with a larger water depth of the flat seabed (**Figure 14(d)**). In addition, regarding the seabed slope, the effect of the change in the seabed slope is equivalent to that of the combination of several flat seabeds as in [7]. Thus, the water depth and seabed slope of the sand deposition area play an important role in the development of a sand spit or a barrier.

4. Numerical simulation of deformation of sandbar formed at the tip of Futtsu cusped foreland

4.1 Change in sandbar offshore of Futtsu Point owing to the 2011 Great Tsunami

Large topographic changes were first discovered by a field observation on June 11, 2011, at the tip of Futtsu Point (**Figure 18**) [9]. Because a tsunami with 2 m height, which was recorded in the field observation at the south shore of Futtsu Point, hit the foreland on March 11, 2011, the sandbar at the tip of Futtsu Point was discharged by the overflow of this tsunami. The impact of the tsunami to the sandbar can be seen in aerial photographs taken on February 3, 2011, and March 27, 2012, before and after the tsunami, respectively (**Figure 19**). Before the tsunami, a slender, concave sandbar extended from Futtsu Point to Dai-ichikaiho Island. On March 27, 2012, almost all of the sandbar was disintegrated by the tsunami overflow, resulting in the submergence of the sandbar and leaving a small sandbar at the tip of Futtsu Point [9]. Comparing the broken line in **Figure 19(b)**, which shows the shapes of the sandbar before the tsunami and the submerged sandbar on March 27, 2012, it is seen that the sand comprising the sandbar was transported northward, implying that the sandbar was flushed away. In addition, part of the sand was transported by the return flow near the tip of the cusped foreland.

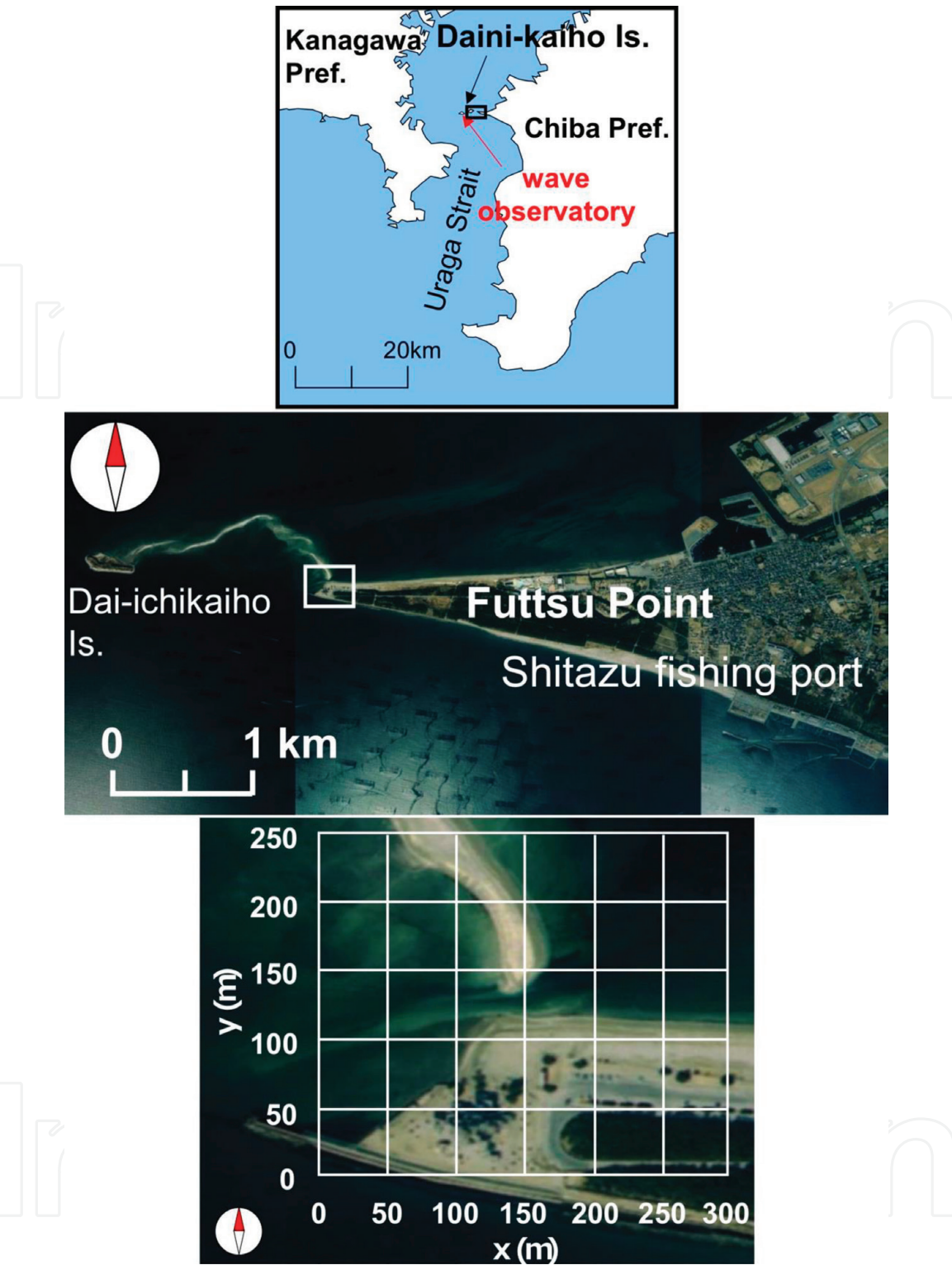


Figure 18.
Location of the study area at the tip of Futtsu Point and coordinate system [9].

4.2 Method of field observation

A rectangular observation area was set up at the tip of Futtsu Point (**Figure 18**), and the shoreline changes in this area were measured using a GPS between June 11, 2011 and October 16, 2012. The shoreline position was measured when the tide level was approximately equal to MSL. The changes in shoreline position were investigated using coordinates (x, y) with reference to a point in the vicinity of the seawall at the tip of Futtsu Point (**Figure 18**), and the berm height and foreshore slope were

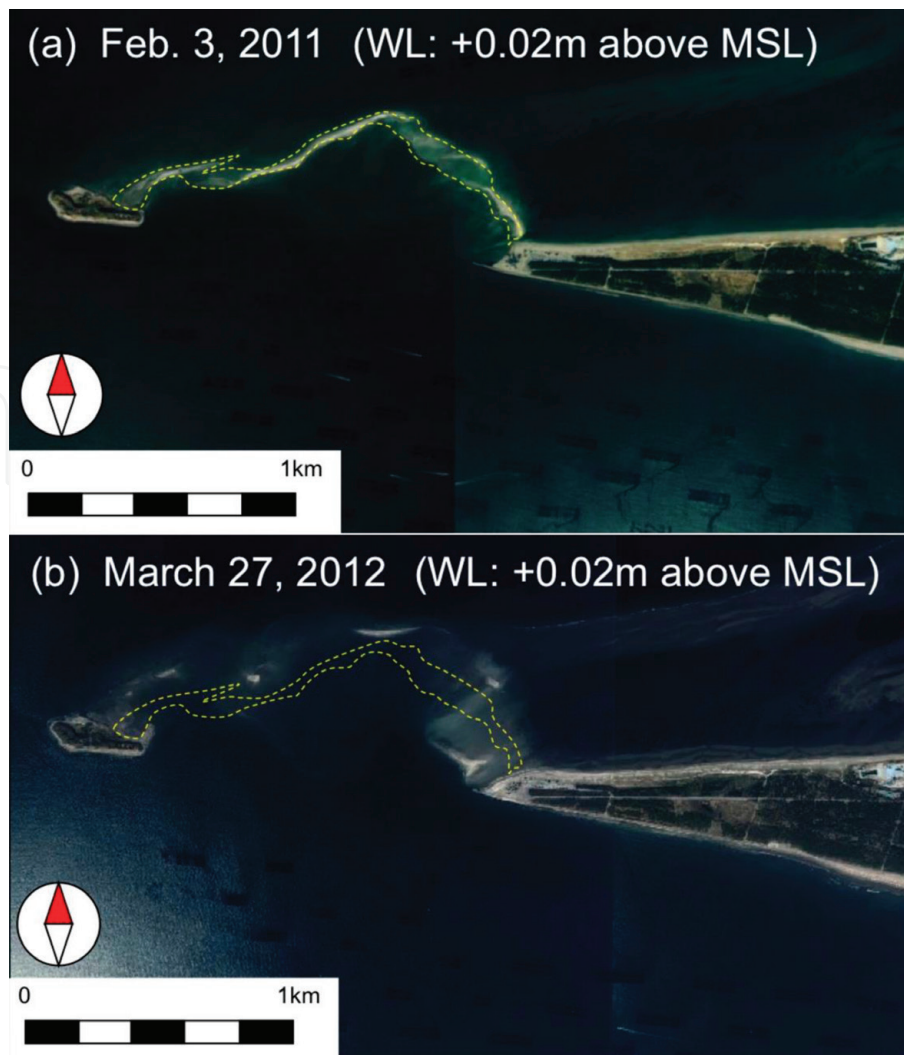


Figure 19.
Aerial photographs of Futtsu Point taken on February 3, 2011, before the tsunami, and March 27, 2012, after the tsunami [9].

measured during low tide on February 26, 2012; the measured berm height was +0.97 m above MSL, and the foreshore slope was 1/8. Wave conditions were investigated using wave observation results offshore of Dainikaiho Island located 2.4 km west of Dai-ichikaiho Island (**Figure 18**).

4.3 Results of field observation

Due to the wave observation offshore of Dainikaiho Island, the wave height normally ranges between 0.3 m in summer and 1 m in winter, and the wave period changes between 3 and 5 s. The important effect upon the deformation of the sandbar at the tip of Futtsu Point is caused by the oblique wave incidence. Monthly changes in wave direction show that predominant wind directions are NNW and SSW, but waves incident from SSW do not affect the beach changes located on the north side of the cusped foreland, because Futtsu Point extends in the E-W direction. Thus, the deformation of the sandbar primarily depends on the waves incident from NNW.

Figure 20 shows an oblique photograph of a crescent-shaped sandbar formed on the north side on Futtsu Point, taken from an observation tower at the tip of Futtsu Point on June 11, 2011 [9]. The shoreline on the west side of the sandbar

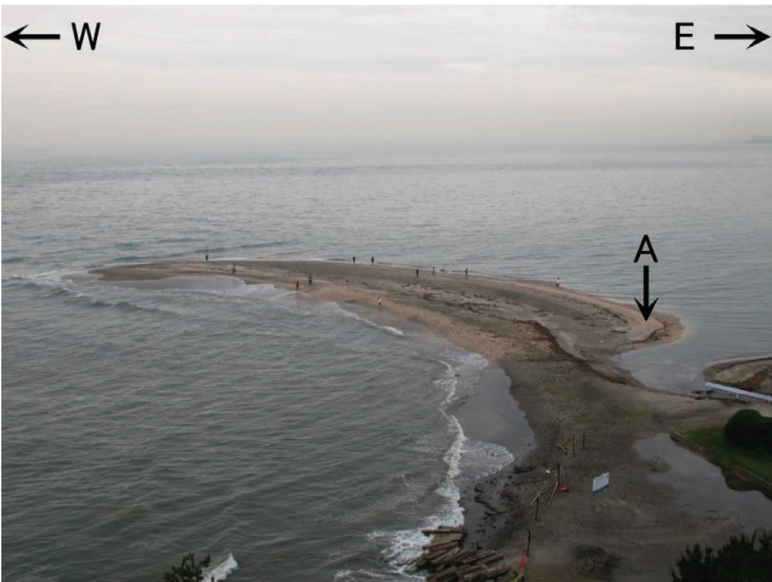


Figure 20.
Oblique photograph of a crescent-shaped sandbar [9].



Figure 21.
Concave shoreline and a sand spit mainly composed of shells [9].

was concave, whereas sand spit A was formed at the east end. **Figure 21** shows a sand spit mainly composed of shells, as denoted by arrow A in **Figure 20**, formed by eastward longshore sand transport along the shoreline of the crescent-shaped sandbar, and the concave shoreline on the lee of the sand spit.

The successive change in shoreline position of this sandbar between June 11, 2011 and February 17, 2012 can be summarized in **Figure 22**. Up to June 11, when the observation began, a crescent-shaped sandbar of 130 m length had developed northward with a concave shoreline on the west side [9]. By July 19, the tip of the sandbar had retreated. Then, the west end of the sandbar was eroded, because wind waves were incident from NNW in July, and the eroded sand was transported eastward, turning around the tip of the sandbar. By September 14, the sandbar had further inclined eastward, and a sand spit was formed on the east side until October 14. After October 14, the entire sandbar eroded out, reducing

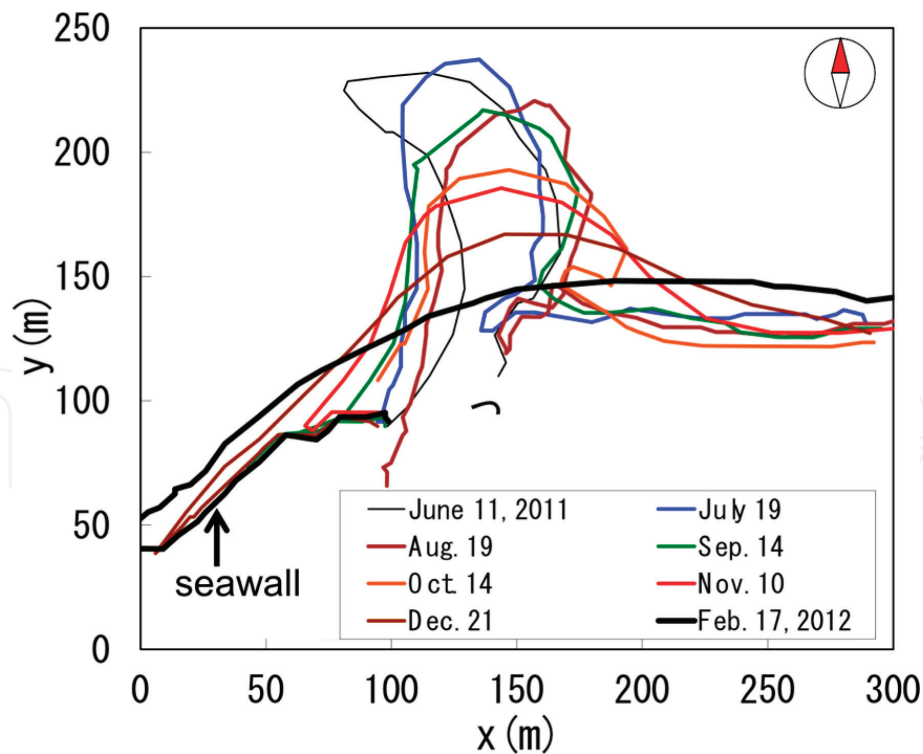


Figure 22.
 Overall changes in sandbar between June 11, 2011, and February 17, 2012 [9].

to a sandbar with a smooth shoreline, and diffusion-type shoreline changes occurred. By February 17, a gradually curved shoreline had formed, and the seawall was buried again by sand.

4.4 Numerical simulation using Type 3 BG model

4.4.1 Calculation conditions

Referring to the results of wave observations between June 2011 and January 2012 offshore of Dainikaiho Island (**Figure 18**), we assumed a mean significant wave height of $H_i = 0.5$ m ($T = 4$ s). The wave direction and directional spreading parameter S_{\max} [15] were determined using a trial-and-error method, so that the measured and calculated shoreline configurations were in good agreement, taking the predominant wave direction of NNW into account [9]. The adopted best-fit wave direction and S_{\max} were N17°W and 2, respectively. h_R was assumed to be 1.1 m, as obtained in the field observation on June 11, 2011, and the depth of closure was assumed to be $h_c = 4H$, where H is the local wave height. The equilibrium slope and the slope of the angle of repose were assumed to be 1/7 and 1/2, respectively. As the initial topography, the sandbar topography measured on July 19, 2011, was assumed, when the shoreline configuration was measured in full scale. Because only the shoreline position was measured in the observation, a uniform beach with a foreshore slope of 1/7 was assumed between heights of 1.1 and -2 m. **Table 3** summarizes the conditions for calculating the deformation of a sandbar.

4.4.2 Calculation results

Figure 23 shows the results [9]. Although the initial sandbar on July 19 had a 50 m width and protruded northward by 100 m (**Figure 23(a)**), two protrusions had formed on both sides of the sandbar by August 19 owing to the wave action

Calculation method	Type 3 BG model
Wave conditions	Incident waves: $H_I = 0.5$ m, $T = 4$ s Wave direction $\theta_W = +17.5^\circ$ (N17.5°W)
Tide level	MSL, 0.0 m
Berm height	$h_R = 1.1$ m
Depth of closure	$h_c = 4H$ (H : wave height at a local point)
Equilibrium slope	$\tan\beta_c = 1/7$
Coefficients of sand transport	Coefficient of longshore sand transport $K_s = 2 \times 10^{-3}$ Coefficient of sand transport by Ozasa and Bampton [12] term $K_2 = 1.62 K_s$ Coefficient of cross-shore sand transport $K_n = 0.2 K_s$
Mesh sizes	$\Delta x = \Delta y = 5$ m
Time intervals	$\Delta t = 1.2$ hr
Total time steps	1×10^4 steps (500 days)
Boundary conditions	Seaward and shoreward ends, $q_x = 0$; right and left ends, $q_y = 0$
Calculation of wave field	Energy balance Equation [13] <ul style="list-style-type: none">• Term of wave dissipation due to wave breaking: Dally et al. [14] model• Wave spectrum of incident waves: directional wave spectrum density obtained by Goda [15]• Total number of frequency components $N_F = 1$• Number of directional subdivisions $N_\theta = 8$• Directional spreading parameter $S_{\max} = 2$• Coefficient of wave breaking $K = 0.17$ and $\Gamma = 0.3$• Imaginary depth between depth h_0 and berm height h_R, 0.5 m• Lower limit of h in terms of wave decay Φ due to wave breaking, $h_{\min} = 0.5$ m• Wave energy = 0 where $Z \geq h_R$

Table 3.
Conditions for calculating deformation of a sandbar.

from N17°W (**Figure 23(b)**). The calculation result that a small embayment on the eastern foot of the sandbar was enclosed by the sand spit is in agreement with the observed shoreline. However, there is some discrepancy between the measured and observed shorelines in that the measured shoreline is straight on the west side of the sandbar, whereas the calculated shoreline has a small protrusion.

By September 14, the shoreline of the north part of the sandbar significantly retreated with a large inclination toward the east, and the shoreline on the east side was connected by a smooth line with a small hollow (**Figure 23(c)**). By October 14, the shoreline in the north part had markedly retreated, and a sand spit had begun to form on the east side (**Figure 23(d)**). By November 10, the sand spit had elongated and became connected to the other shore, resulting in the formation of a gradually curved shoreline because of the continuous sand supply from the upcoast (**Figure 23(e)**). The protruding sandbar had eroded to form a gradually curving shoreline by December 21, 2011 (**Figure 23(f)**). Thus, the changes in the sandbar that was formed by the 2011 Great East Japan Earthquake tsunami were well predicted using the Type 3 BG model. Also, the subsequent deformation of the sandbar was found to be due to the action of waves incident from the direction of N17°W [9].

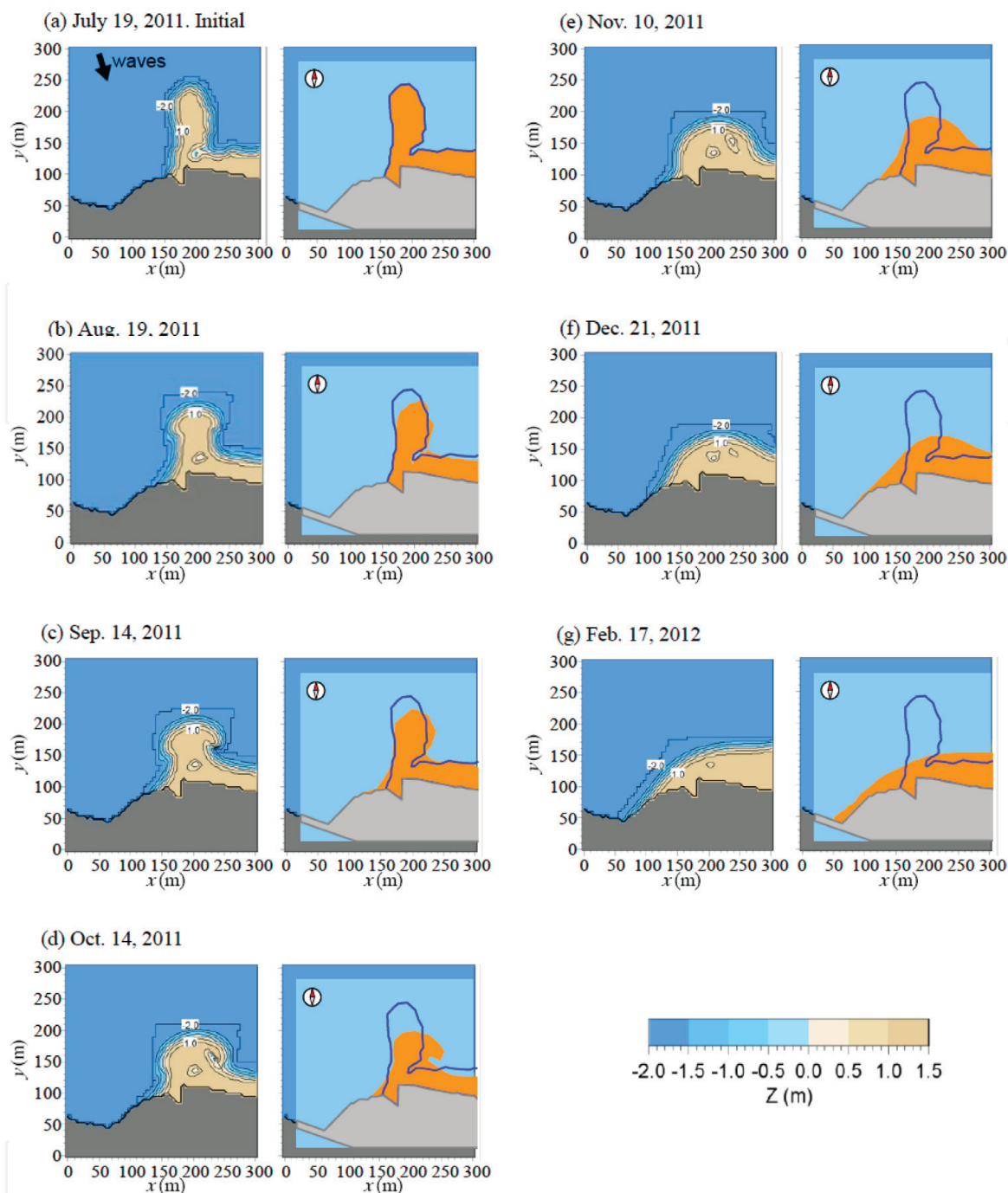


Figure 23.
Calculation results of deformation of sandbar [9].

5. Conclusions

In Chapter 5, three topics were discussed, and topographic changes were predicted using the BG model: (1) formation of a bay barrier in flat shallow sea and merging of bay mouth sand spits (Type 5 BG model), (2) elongation of sand spit on seabed with different water depths (Type 3 BG model), and (3) deformation of a sandbar formed at the tip of the Futtsu cusped foreland owing to a tsunami which propagated into Tokyo Bay after the Great East Japan Earthquake (Type 3 BG model).

1. The elongation and merging of sand spits formed at a bay mouth of symmetric or asymmetric shape were studied. When a slender sandy headland was placed on the left side of the bay (Case 1), sand spits independently developed near the tip

and the base of the sandy headland at the initial stage. With increasing size of the sand spit formed near the tip of the sandy headland, the wave-sheltering effect increased, and the sand spits that had formed near the base of the sandy headland were subject to the wave-sheltering effect and disappeared. Finally, a single sand spit elongated rightward. The simulation results for the elongation of a single sand spit into a bay and an image in Zenkovich [4] were in good agreement.

2. When double sandy headlands were placed in the calculation domain (Case 2), a bay barrier with a concave shape was formed with a wide beach in the central part of the bay barrier. When the sandy headlands were placed asymmetrically (Case 3), the wave-sheltering effect of the sand spit from the larger headland on the smaller sand spit was significant, and the sand spits merged with each other to form a single bay mouth barrier. In Case 4, the formation of the embayed coasts by the extension of a barrier island as described in Zenkovich [4] was predicted, and the calculation results were in good agreement with the explanation regarding the formation of the embayed coasts given by Zenkovich [4].
3. The development of the sand spit was remarkable with a smaller water depth of the sand deposition zone, because sufficient wave energy cannot penetrate into the shallow body of water. In contrast, sufficient wave energy can reach the shoreline with a larger water depth, resulting in the increase in the curvature of the shoreline.
4. A crescent-shaped sandbar was formed offshore of the Futtsu cusped foreland by the overflow during the 2011 Great East Japan Earthquake tsunami. The subsequent shoreline changes due to wind waves were investigated by field observation. These topographic changes were studied using the Type 3 BG model. The predicted and measured topographic changes of the crescent-shaped sandbar were in good agreement.

As further applications of the Type 3 BG model, (1) the model was used to predict the elongation of sand spit and profile changes on sloping shallow seabed under waves [16], (2) field observation on the formation of a barrier island as a result of elongation of sand spit was studied in Nabeshima area facing Nakatsu tidal flat in the Suonada Sea, and their formation was numerically predicted using the Type 3 BG model [17]. (3) The deformation of an isolated offshore sandbar on tidal flat and merging with beach owing to waves was also predicted using the Type 3 BG model in [18]. As regard the formation of a sand spit at the river mouth, (4) the rapid formation of a sand spit at a river mouth was measured at the Shimanto River mouth, and the deformation of a sand spit was predicted using Type 3 BG model in [19]. Moreover, (5) the beach changes on a coral cay owing to waves with seasonal change in wave direction was investigated on Embudu Village Island in the Maldives, and the seasonal movement of sand spits was predicted using the Type 3 BG model in [20].

Acknowledgements

Parts of the work described in Chapter 5, i.e., numerical simulations of elongation and merging of bay mouth sand spits, elongation of sand spit on seabed with different water depths, and deformation of sandbar formed at the tip of Futtsu cusped foreland by the 2011 tsunami, were based on the conference papers [5, 7, 9], respectively, presented at the 34th Conference on Coastal Engineering in 2014. We would like to express our gratitude for the use of materials.

IntechOpen

Author details


Takaaki Uda^{1*}, Masumi Serizawa² and Shiho Miyahara²

1 Public Works Research Center, Tokyo, Japan

2 Coastal Engineering Laboratory Co., Ltd., Tokyo, Japan

*Address all correspondence to: uda@pwrc.or.jp

IntechOpen

© 2018 The Author(s). Licensee IntechOpen. Distributed under the terms of the Creative Commons Attribution - NonCommercial 4.0 License (<https://creativecommons.org/licenses/by-nc/4.0/>), which permits use, distribution and reproduction for non-commercial purposes, provided the original is properly cited. 

References

- [1] Schwarz ML. The multiple causation of barrier islands. *Journal of Geology*. 1971;**79**:91-93
- [2] Nummedal D. Barrier Islands. In: Komar PD, editor. *Handbook of Coastal Processes and Erosion*. Boca Raton, FL: CRC Press; 1983. pp. 77-121
- [3] Bird E. *Coastal Geomorphology: An Introduction*. New York: John Wiley and Sons; 2000. p. 322
- [4] Zenkovich VP. *Processes of Coastal Development*. New York: Interscience Publishers, Div. of John Wiley and Sons, INC; 1967. p. 751
- [5] Watanabe S, Uda T, Serizawa M, Miyahara S. Numerical simulation of elongation and merging of bay mouth sand spits using the BG model. In: *Proceedings of 34th ICCE*; 2014. pp. 1-11. https://journals.tdl.org/icce/index.php/icce/article/view/7105/pdf_409
- [6] Serizawa M, Uda T. Prediction of formation of sand spit on coast with sudden change in coastline using improved BG model. In: *Proceedings of the Coastal Sediments*; 2011. pp. 1907-1919
- [7] San-nami T, Uda T, Serizawa M, Miyahara S. Numerical simulation of elongation of sand spit on seabed with different water depth and slopes. In: *Proceedings of 34th ICCE*; 2014. pp. 1-13. https://journals.tdl.org/icce/index.php/icce/article/view/7112/pdf_415
- [8] Uda T, Kanda Y. Beach erosion of Futtsu Point in Chiba Prefecture. *Coastal Engineering Journal, JSCE*. 1995;**42**:651-655. (in Japanese)
- [9] Kobayashi A, Uda T, Serizawa M, Miyahara S, Endo M. Numerical simulation of deformation of sandbar formed at tip of Futtsu cusplate foreland by the 2011 Tsunami. In: *Proceedings of 34th ICCE*; 2014. pp. 1-11. https://journals.tdl.org/icce/index.php/icce/article/view/7111/pdf_479
- [10] Uda T. *Japan's Beach Erosion—Reality and Future Measures*. 2nd ed. Vol. 530. Singapore: World Scientific; 2017
- [11] Ashton A, Murray AB. High-angle wave instability and emergent shoreline shapes: 1. Modeling of sand waves, flying spits, and capes. *Journal of Geophysical Research*. 2006;**111**:F04011. DOI: 10.1029/2005JF000422
- [12] Ozasa H, Brampton AH. Model for predicting the shoreline evolution of beaches backed by seawalls. *Coastal Engineering*. 1980;**4**:47-64
- [13] Mase H. Multidirectional random wave transformation model based on energy balance equation. *Coastal Engineering Journal, JSCE*. 2001;**43**(4):317-337
- [14] Dally WR, Dean RG, Dalrymple RA. A model for breaker decay on beaches. In: *Proceedings of 19th ICCE*; 1984. pp. 82-97. <https://journals.tdl.org/icce/index.php/icce/article/view/3787/3470>
- [15] Goda Y. *Random Seas and Design of Maritime Structures*. Vol. 323. Tokyo: University of Tokyo Press; 1985
- [16] Miyahara S, Uda T, Serizawa M, San-nami T. Elongation of sand spit and profile changes on sloping shallow seabed. In: *8th International Conference on Asian and Pacific Coasts (APAC 2015)*. *Procedia Engineering*. 2015;**116**:245-253
- [17] Miyahara S, Uda T, Serizawa M. Field observation and numerical simulation of barrier island formation

as a result of elongation of sand spit and its attachment to opposite shore. In: Proceedings of 35th Conference on Coastal Engineering, Sediment 5; 2016. pp. 1-14. <https://icce-ojs-tamu.tdl.org/icce/index.php/icce/article/view/8103/pdf>

[18] San-nami T, Uda T, Miyahara S, Serizawa M. Deformation of an isolated offshore sandbar on tidal flat and mergence with beach due to waves, Coastal Sediments '15, CD-Rom, No. 14; 2015. pp. 1-14

[19] Serizawa M, Uda T, Miyahara S. Rapid formation of a sand spit at river mouth and its prediction using BG model. In: Proceedings of 9th International Conference on Asian and Pacific Coasts (APAC2017); 2017. pp. 479-490

[20] Uda T, Serizawa M, Miyahara S. Seasonal movement of sand spits on a coaral cay of Embudu Village Island in the Maldives. In: Proceedings of 9th International Conference on Asian and Pacific Coasts (APAC2017); 2017. pp. 467-478